

Organic & Biomolecular Chemistry

Accepted Manuscript



This article can be cited before page numbers have been issued, to do this please use: L. Wang, G. Zhu, Q. Zhang, C. Duan, Y. Zhang, Z. Zhang, Y. Zhou, T. Lu and W. Tang, *Org. Biomol. Chem.*, 2017, DOI: 10.1039/C7OB00518K.



This is an Accepted Manuscript, which has been through the Royal Society of Chemistry peer review process and has been accepted for publication.

Accepted Manuscripts are published online shortly after acceptance, before technical editing, formatting and proof reading. Using this free service, authors can make their results available to the community, in citable form, before we publish the edited article. We will replace this Accepted Manuscript with the edited and formatted Advance Article as soon as it is available.

You can find more information about Accepted Manuscripts in the [author guidelines](#).

Please note that technical editing may introduce minor changes to the text and/or graphics, which may alter content. The journal's standard [Terms & Conditions](#) and the ethical guidelines, outlined in our [author and reviewer resource centre](#), still apply. In no event shall the Royal Society of Chemistry be held responsible for any errors or omissions in this Accepted Manuscript or any consequences arising from the use of any information it contains.

Rational design, synthesis, and biological evaluation of Pan-Raf inhibitors to overcome resistance

Lu Wang^a, Gaoyuan Zhu^a, Qing Zhang^b, Chunqi Duan, Yanmin Zhang^a, Zhimin Zhang^a, Yujun Zhou^a, Tao Lu^{a,c*}, Weifang Tang^{a,*}

^a School of Basic Science, China Pharmaceutical University, 639 Longmian Avenue, Nanjing, Jiangsu 211198, China.

^b School of Basic Medicine and Clinical Pharmacy, China Pharmaceutical University, 639 Longmian Avenue, Nanjing, Jiangsu, 211198, China.

^c State Key Laboratory of Natural Medicines, China Pharmaceutical University, 24 TongjiXiang, Nanjing, Jiangsu 210009, China.

Abstract: Selective BRaf^{V600E} inhibitors with DFG-in conformation have been proven effective against a subset of melanoma. However, representative inhibitor vemurafenib rapidly acquire resistance in the BRaf^{WT} cells through a CRaf or BRaf^{WT} dependent manner. Simultaneous targeting all subtypes of Raf proteins offer the prospect of enhanced efficacy as well as reduced potential for acquired resistance. Described herein is the design and characterization of a series of compounds **I-01~I-22** which based on pyrimidine scaffold with DFG-out conformation as Pan-Raf inhibitors. Among them, **I-15** binds to all Raf protomers with IC₅₀ values of 12.6 nM (BRaf^{V600E}), 30.1 nM (ARaf), 19.7 nM (BRaf^{WT}) and 17.5 nM (CRaf), respectively, demonstrates cellular activity against BRaf^{WT} phenotypic melanoma and BRaf^{V600E} phenotypic colorectal cancer cells. The western blot results for the P-Erk inhibition in human melanoma SK-Mel-2 cell line showed **I-15** inhibited the proliferation of SK-Mel-2 cell line at concentration as low as 400 nM, without paradoxical activation of Erk as vemurafenib, which supported **I-15** may become a good candidate compound to overcome the resistance of melanoma induced by vemurafenib. **I-15** also have a favorable pharmacokinetic profile in rat. Rational design, synthesis, SAR, lead selection and evaluation of the key compounds studies are described.

Keywords: Pan-Raf inhibitors; cyclopropyl formamide; resistance

1. Introduction

The Ras-Raf-Mek-Erk (mitogen-activated protein kinase MAPK) cascade is a central signaling component that plays a role in the initiation and regulation of most of the stimulated cellular processes such as proliferation, survival and differentiation.¹ As a downstream effector of Ras in the MAPK signaling pathway, Raf proteins are cytosolic protein kinases that regulate cell responses to extracellular signals.² There are three Raf proteins in cells, ARaf, BRaf and CRaf, and studies have shown that the formation of complexes by these different isoforms has an important role in their activation.³⁻⁵ BRaf, unlike ARaf or CRaf, can be converted into an active oncogenic protein BRaf^{V600E} (Val⁶⁰⁰-Glu⁶⁰⁰, V600E) by single-point mutation. This substitution mimics phosphorylation of the activation loop, elevating the in vitro enzymatic activity by up to 500~700-fold compared with its wild-type counterpart.⁶ According to the binding modes of DFG (a conserved amino acid sequence of D594, F595 and G596), which derived from crystallographic analysis, Raf kinase inhibitors were categorized into two types, DFG-out and DFG-in series.⁷ The DFG-out inhibitors, such as sorafenib⁸ and LY3009120,⁹ engage the protein in DFG-out conformation and inhibit all subtypes of Raf proteins (Figure 1). The DFG-in inhibitors, such as vemurafenib, bind to the ATP binding site of the kinase with a DFG-in conformation and inhibits BRaf^{V600E} with high selectivity.¹⁰

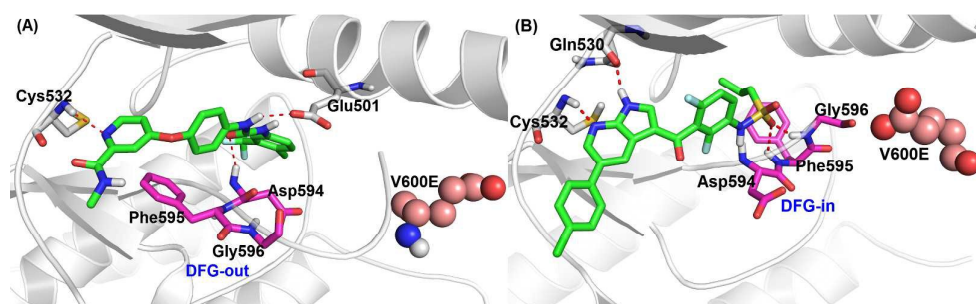


Figure 1. Binding mode of BRaf^{V600E} (A) DFG-out conformation for PDB 1UWJ (crystalized with sorafenib) (B) DFG-in conformation for PDB 3OG7 (crystalized with vemurafenib)

Vemurafenib have shown significant clinical efficacy in melanoma patients

harboring B Raf^{V600E}.¹¹⁻¹³ However, after 6 months, the development of acquired resistance (the resistance caused by vemurafenib) is reported as a well-known side effect. The mechanism for acquired resistance remains complicated. In cells, wild type Raf kinases signal as dimers comprising various ARaf, B Raf, and CRaf homodimers or heterodimers. The binding mode of inhibitors like vemurafenib (and others which cause paradoxical activation) fail to occupy both protomers of these cellular dimers. Furthermore, the binding of vemurafenib and analogous inhibitors to a cellular B Raf protomer conformationally transactivates the unbound protomer (usually CRaf or another B Raf) to increased enzymatic activity and downstream signaling through ERK.¹⁴⁻¹⁶ Pan-Raf inhibitors can bind to cellular Raf dimers and occupy both protomers of these dimers (Figure 2).

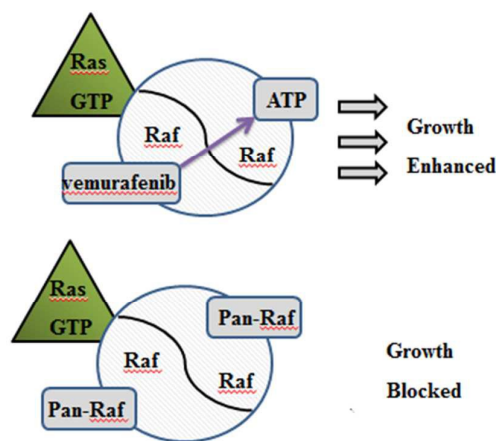


Figure 2. The mechanism of acquired resistance

About 20% of patients had intrinsic resistance and didn't respond to the drug despite the presence of B Raf^{V600E}.¹⁷ Ras mutant-driven cancers signal through B Raf/CRaf heterodimers, and that a Pan-Raf inhibitor capable of inhibiting these cellular forms would find utility in the treatment of Ras mutant driven cancers, comprising approximately 1/3 of human cancers.¹⁸⁻²⁰ Clinically, paradoxical activation promotes drug induced skin lesions including keratoacanthomas and squamous cell carcinoma.^{12, 13}

It is demonstrated that the feedback activation in B Raf^{WT} bearing cancers can be significantly suppressed by DFG-out Raf inhibitors.²¹ The optimal Raf inhibitor should be DFG-out type that preserves potency against oncogenic B Raf^{V600E} without

driving activation of BRaf^{WT} or CRaf.^{22, 23} Hence we develop a series of DFG-out conformation pyrimidine derivatives **I-01~I-22** having Pan-Raf potency with low IC₅₀ values, they without agonistically affect the MAPK pathway in BRaf^{WT} extraordinary expression melanoma cell line (The data were obtained on compound **I-14~I-15**). Furthermore, the compounds also displayed inhibition on the proliferation of a panel of vemurafenib-resistant cancer cells harboring overexpressed BRaf^{V600E} (A375: WB assay, acquired resistance; COLO-205: IC₅₀ = 1.92 μM, SK-Mel-2: IC₅₀ = 0.58 μM, intrinsic resistance), representing new leads for further development of Pan-Raf inhibitors to overcome the resistance caused by vemurafenib.

2. Results and discussion

These compounds were evaluated with enzyme and cell-based assay. Furthermore, SAR (structure-activity relationship) had also been established. **I-14** and **I-15** with optimal potency at enzymatic as well as cellular level was chosen to study the possible biological mechanisms. **I-15** achieving solubility of 0.228 mg/mL was also studied some pharmacokinetic profiles compared to **Y-1**.

2.1. Inhibitors design and molecular modeling

Previously, lead compound **Y-1** is found as a BRaf^{V600E} inhibitor with enzymatic activity (IC₅₀ = 3.2 nM) and antiproliferative activity against cell line A375 (IC₅₀ = 8.8 μM).²⁴ However, its solubility and chemical novelty still need to be improved (Figure 4). Thus, on the basis of the fragment-based approach²⁵ which decomposes compounds from several databases, we tried to recombine those fragments by the retrosynthetic combinatorial analysis procedure (RECAP) algorithm.²⁶ Databases consist of those novel compounds were again decomposed into fragments by the fragment-based approach,²⁵ which may greatly improve the novelty of the chemical space for the databases. Fragments generated in this way were then docked to the active binding site. A 1-(2-(methylamino)pyrimidin-4-yl)-N- phenylcyclopropane-1-carboxamide (the red colored part of **I-01** as shown in Figure 3) was found to be in great alignment with the N-phenyl-3-(9H-purin-6-yl) pyridin-2-amine part of the lead **Y-1** (Figure 3A) as well as the crystalized ligand of PDB 3IDP (BRaf^{V600E} IC₅₀ = 1.6 nM) (Figure 3B). Furthermore, **I-01** was designed by combining the novel scaffold

with lead **Y-1** through a scaffold-merging strategy. As shown in Figure 3C and Figure 3D, **I-01** adopts a similar binding conformation with lead **Y-1** and the crystalized ligand of PDB 3IDP, which maintains with the original essential hydrogen bonds in both the hinge region and the DFG part. The cyclopropyl formamide part overlaps well with pyridine moiety occupying this small hydrophobic binding pocket omitted in the binding conformation of sorafenib.

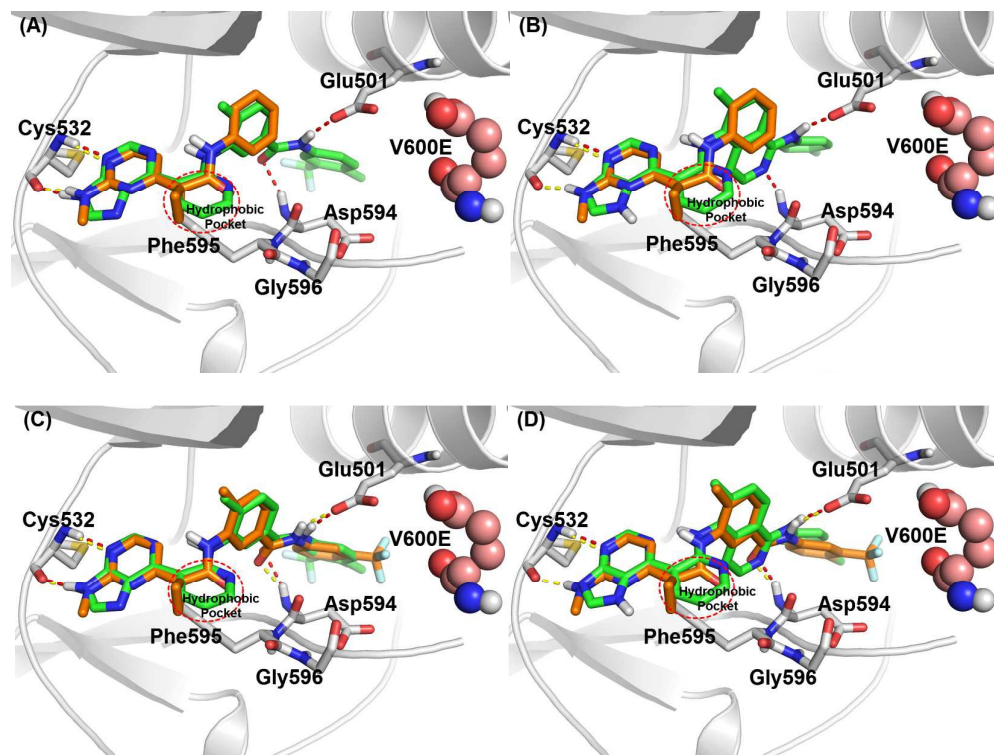


Figure 3. The binding conformation of the novel scaffold and **I-01**

Alignment of lead scaffold and **I-01** with **Y-1** and the crystalized ligand of PDB 3IDP (3A) Alignment of lead scaffold of **I-01** (orange colored carbons) with **Y-1** (green colored carbons). (3B) Alignment of lead scaffold of **I-01** with crystallized ligand (green) from PDB 3IDP. (3C/D) Fully elaborated structures from lead scaffold of **I-01**, showing further overlap in the back hydrophobic pocket.

The structure shown for **Y-1** is a docked structure, and not an actual co-crystal structure. The structures of **I-01**–**I-22** were shown in the same manner to **Y-1**.

However, **I-01** didn't display comparable enzymatic activities with **Y-1** or the ligand of PDB 3IDP (Figure 4). Hence the structure optimization was performed to

identify potent compounds.

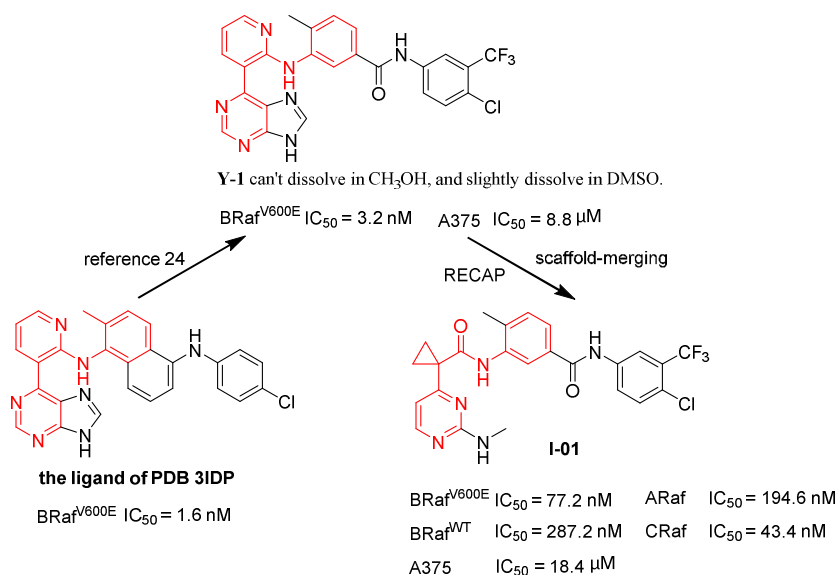


Figure 4. The structure modification of **Y-1** to **I-01**

Before optimizing the lead **I-01**, we explored the binding mode of **I-01**. The modeled binding mode of **I-01** to the DFG-out conformation of BRaf^{V600E} revealed that **I-01** binds to the BRaf^{V600E} ATP binding pocket with the pyrimidine core forming two essential hydrogen bonds with the hinge region Cys532 (Figure 5). In addition to these hydrogen bonds, the amide group forms two hydrogen bonds with Asp594 and Glu501. Then, we turned our attention toward the methylamino group proximal to the pyrimidine core. The binding mode showed it to form hydrophilic interactions with the surrounding amino acid residues. More importantly, the methylamino group in the pyrimidine ring was directed toward the solvent accessible region of BRaf^{V600E} (Figure 5). The chlorine atom in the terminal phenyl ring was directed toward another solvent accessible region, too. In order to get a better occupation of these two solvent accessible regions, we started optimization program to modify **I-01** with an aim to improve solubility and cellular potency.

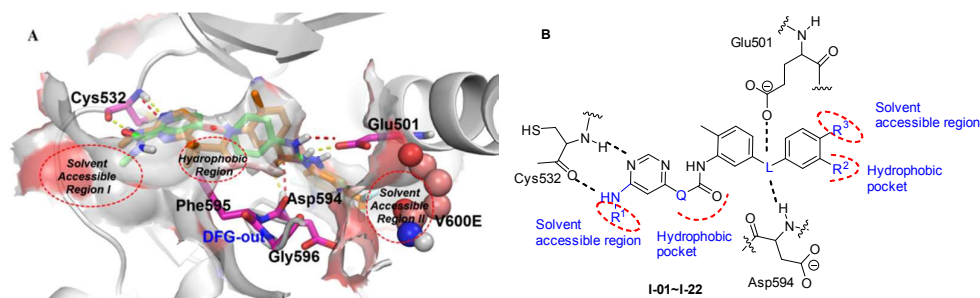


Figure 5. (A) The binding pockets of BRAF^{V600E}. (B) The binding mode of **I-01~I-22** and sorafenib.

The further modification depended on the important structural features essential for enzymatic activity. L as linkage using different groups was attempted. Fragment Q was investigated on rigid and steric factors. R¹ substituent was directed toward the solvent accessible region of BRAF^{V600E} proximal to the hinge region. R² substituent was exposed to the hydrophobic back pocket, which was formed by a rearrangement of the activation loop and subsequent movement of a phenylalanine side chain of DFG loop.²⁷ R³ substituent in the terminal phenyl ring was directed toward another solvent accessible region of BRAF^{V600E}. Based on these information, we described the design and synthesis of pyrimidine derivatives **I-01~I-22** as new DFG-out BRAF^{V600E} inhibitors.

2.2. Chemistry

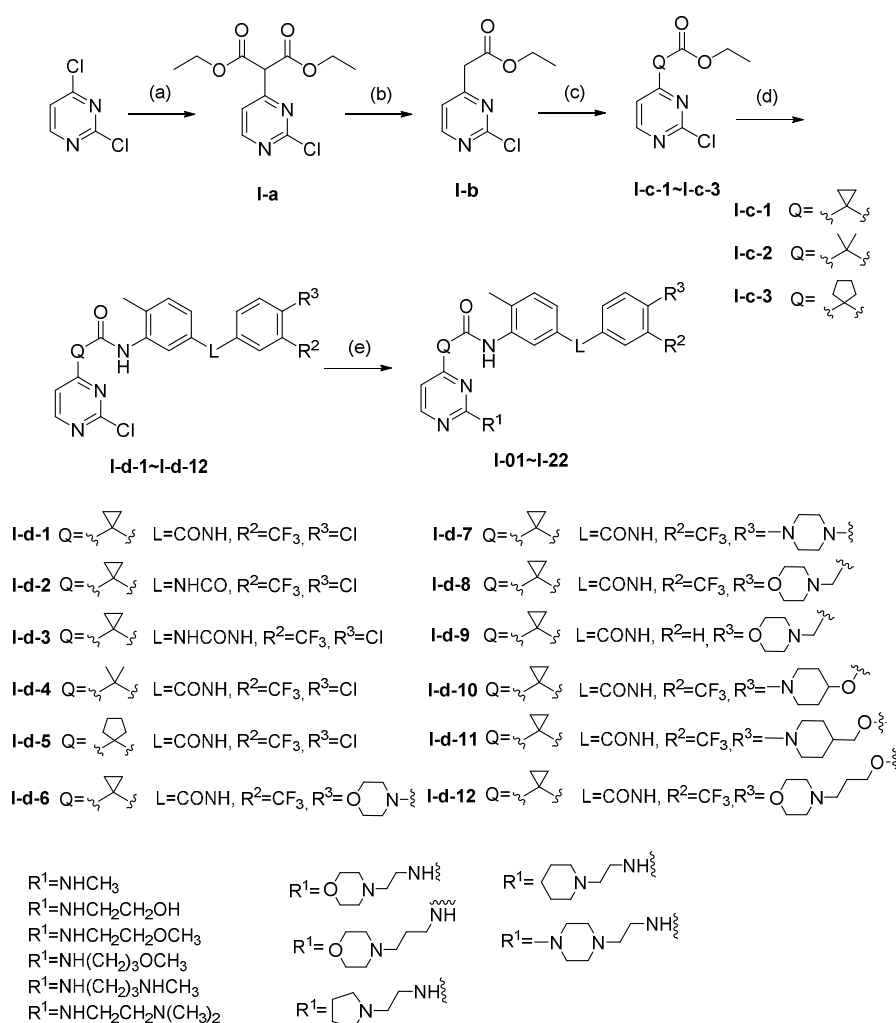
As summarized in Scheme 1, totally 22 compounds were synthesized. The synthetic routes were illustrated in Scheme 1–3. The chemical structures of these compounds were confirmed by ¹H-NMR, ¹³C-NMR, HRMS spectra and results were presented in experimental section.

The target pyrimidine derivatives **I-01~I-22** were prepared by the method shown in Scheme 1. The reaction of commercially available 2, 4-dichloropyrimidine with diethyl malonate in the presence of sodium hydride gave diethyl 2-(2-chloropyrimidin-4-yl) malonate **I-a**. The prepared **I-a** was allowed to react with sodium ethoxide to afford the desired **I-b**. Subsequent alkylation of **I-b** with 1, 2-dibromoethane, iodomethane or 1, 4-dibromobutane in the presence of sodium

hydroxide afforded the corresponding alkylated derivatives **I-c-1~I-c-3** in 90.2%, 93.4% or 90.2%, respectively.

Amide-forming reactions of **I-c-1~I-c-3** with the corresponding anilines **A1~A10** were carried out in the presence of trimethylaluminium (2 M solution of toluene) under the condition of nitrogen atmosphere to give **I-d-1~I-d-12** in 75.6–91.4%. Finally, the reaction of **I-d-1~I-d-12** with commercially available amines through S_NAr substitution reaction provided **I-01~I-22** in 80.3–93.1%.

Scheme 1. The synthetic route of **I-01~I-22**



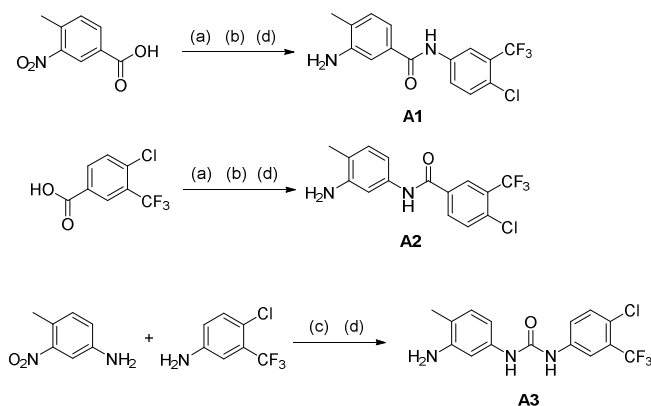
Reagents and conditions: (a) diethyl malonate, NaH, THF, 0°C, 0.5 h, then reflux, 2.5 h; (b) EtONa, EtOH, reflux, 2.5 h; (c) 1,2-dibromoethane, NaOH, DMF, r.t., 5 h, 90.2%; iodomethane, NaOH, DMF, r.t., 5 h, 94.3%; 1,4-dibromobutane, NaOH, DMF, r.t., 5 h, 90.1%; (d) **A1~A10**, Al(CH₃)₃, toluene, nitrogen atmosphere, 80°C, 5 h, 70.8–88.6%; (e) R¹NH₂, DIPEA, EtOH, reflux,

2 h, 80.3–92.7%.

Totally 10 important intermediates **A1–A10** were synthesized according to Scheme 2 and Scheme 3 via a two-five step process.

Intermediates of anilines **A1–A2** were prepared by the method shown in Scheme 2. Substituted benzoyl chloride, which prepared in the presence of benzoic acid with various substituent and oxalyl chloride, were allowed to react with 4-chloro-3-(trifluoromethyl) aniline or 4-methyl-3-nitro-substituted amides to afford the corresponding nitroaniline. Subsequent treatment of the resulting substituted amide with Fe/NH₄Cl gave the corresponding aniline **A1–A2** in 72.6% or 80.4%, respectively. **A3** was generated from condensation reaction using CDI (N,N-carbonyldiimidazole). Then, achieved crude product was converted to **A3** through reduction reaction in 92.6%.

Scheme 2. Synthesis of intermediates **A1–A3**



Reagents and conditions: (a) (COCl)₂, CH₂Cl₂, r.t., 2 h; (b) 4-chloro-3-(trifluoromethyl) aniline or 4-methyl-3-nitroaniline, Et₃N, CH₂Cl₂, r.t., 5 h; (c) CDI, CH₂Cl₂, r.t., 34 h; (d) Fe, NH₄Cl, 75% EtOH, reflux, 3 h.

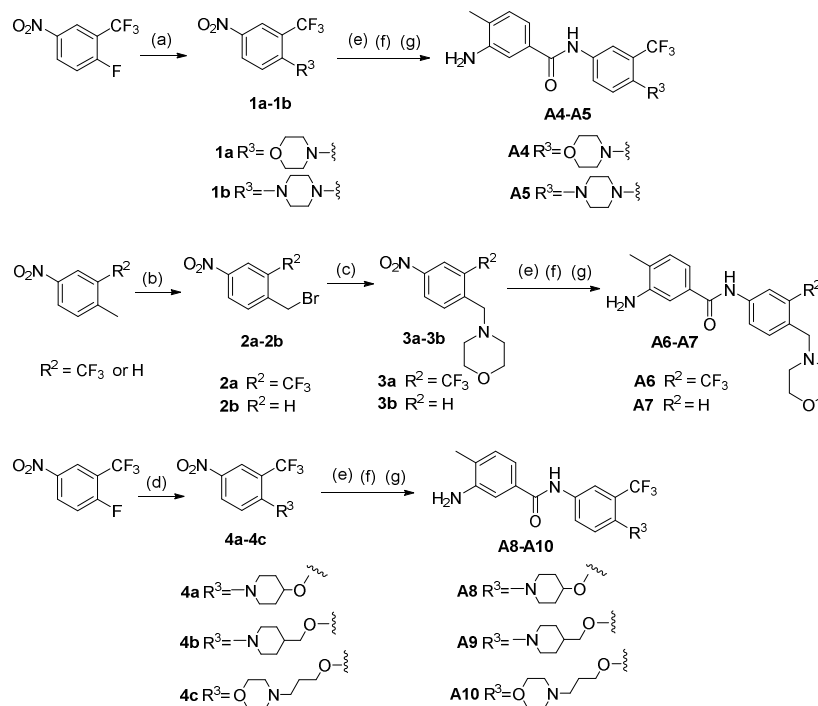
The reaction of 1-fluoro-4-nitro-2-(trifluoromethyl) benzene with morpholine or N-methyl piperazine in solvent DMSO (dimethyl sulfoxide) through S_NAr substitution reaction provided **1a–1b** in 94.2% or 91.4%, respectively (**Scheme 3**). Reduction of the nitro group in **1a–1b** using Fe/NH₄Cl gave the corresponding aniline. Subsequent treatment of the resulting aniline with intermediate 4-methyl-3-nitrobenzoyl chloride

provided substituted amide, was reduced with Fe/NH₄Cl to afford the desired anilines **A4–A5** in 85.4% or 76.2%, respectively.

The desired aniline **A6–A7** utilized 4-nitrotoluene or 4-methyl-3-trifluoromethyl nitrobenzene as starting material. With NBS (N-bromosuccinimide) in solvent DCE (1,2-dichloroethane), they were converted to **2a** or **2b** in 86.4% or 89.2%, respectively. **2a–2b** were converted to **3a–3b** in the presence of NEt₃ as base, THF (tetrahydrofuran) as solvent. The last three steps of **A6–A7** were same as previous reaction (e, f and g) adopted for **A4–A5**.

The reaction of commercially available 1-fluoro-4-nitro-2-(trifluoromethyl) benzene with 1-methylpiperidin-4-ol, (1-methylpiperidin-4-yl) methanol or 3-morpholinopropan-1-ol in the presence of sodium hydride in solvent DMF (N,N-dimethylformamide) gave **4a–4c**. The last three steps were same as previous reaction (e, f and g) adopted for **A4–A5**. Then, the desired intermediates **A8–A10** were afforded in 89.4%, 86.4% or 85.2%, respectively.

Scheme 3. Synthesis of intermediates **A4–A10**



Reagents and conditions: (a) morpholine or N-methyl piperazine, DMSO, 100°C, 5 h, 94.2% or 91.4%; (b) NBS, DCE, reflux, 5 h, 86.4%; (c) morpholine, NEt₃, THF, reflux, 2 h; (d)

1-methylpiperidin-4-ol, (1-methylpiperidin-4-yl) methanol or 3-morpholinopropan-1-ol, NaH, DMF, ice bath, 0.5 h, then 100°C, 5 h; (e) Fe, NH₄Cl, 75% EtOH, reflux, 2 h; (f) 4-methyl-3-nitrobenzoyl chloride, Et₃N, CH₂Cl₂, r.t, 5 h; (g) Fe, NH₄Cl, 75% EtOH, reflux, 2 h.

2.3. Investigation the enzymatic activity of compounds

2.3.1. Compounds screened for solubility and enzymatic activity against B Raf^{V600E}

Newly synthesized compounds were evaluated as B Raf^{V600E} inhibitors using vemurafenib, sorafenib and LY3009120 as reference compounds (vemurafenib and sorafenib have launched, LY3009120 is a Pan-Raf inhibitor). Most of compounds showed IC₅₀ values in the submicromolar range (Table 1).

Table 1. SAR exploration of compounds against B Raf^{V600E} activity

Compd	L	Q	R ¹	R ²	R ³	Solubility	B Raf ^{V600E}	
						mg/mL	activity% ^a	IC ₅₀ (nM) ^c
I-01	CONH		CH ₃	CF ₃	Cl	0.016	7.1	77.2±2.4
I-02	NHCO		CH ₃	CF ₃	Cl	0.015	7.3	166.0±4.6
I-03	NHCONH		CH ₃	CF ₃	Cl	0.009	8.4	154.0±3.1
I-04	CONH		CH ₃	CF ₃	Cl	0.005	92.1	ND ^b
I-05	CONH		CH ₃	CF ₃	Cl	0.005	97.1	ND
I-06	CONH		CH ₂ CH ₂ OH	CF ₃	Cl	0.102	13.6	44.8±11.2
I-07	CONH		CH ₂ CH ₂ OCH ₃	CF ₃	Cl	0.241	3.6	95.7±18.7
I-08	CONH		(CH ₂) ₃ OCH ₃	CF ₃	Cl	0.187	13.3	133.0±17.5
I-09	CONH		CH ₂ CH ₂ NHCH ₃	CF ₃	Cl	0.065	63.2	ND
I-10	CONH		CH ₂ CH ₂ N(CH ₃) ₂	CF ₃	Cl	0.204	9.0	75.3±7.3

I-11	CONH			CF ₃	Cl	0.282	7.7	46.1±21.6
I-12	CONH			CF ₃	Cl	0.243	14.1	73.8±27.7
I-13	CONH			CF ₃	Cl	0.261	11.4	59.6±13.1
I-14	CONH			CF ₃	Cl	0.197	10.5	48.8±7.9
I-15	CONH			CF ₃	Cl	0.228	3.0	12.6±15.8
I-16	CONH		CH ₃	CF ₃		0.214	30.4	ND
I-17	CONH		CH ₃	CF ₃		0.241	35.6	ND
I-18	CONH		CH ₃	CF ₃		0.198	37.7	195.0±9.8
I-19	CONH		CH ₃	H		0.211	94.4	ND
I-20	CONH		CH ₃	CF ₃		0.176	21.7	154.0±16.3
I-21	CONH		CH ₃	CF ₃		0.150	40.0	ND
I-22	CONH		CH ₃	CF ₃		0.203	26.2	144.0±22.2
vemurafenib								31.6±2.4
sorafenib								38.1±3.0
LY3009120								5.5±3.9

^acontrol activity: compounds with concentration of 0.5 μ M; ^b not determination; ^c n=3

Replacement of the amide function of **I-01** with either a “reverse” amide or urea linkage **I-02~I-03** (Table 1), led to at least two-fold reduction in potency. In order to facilitate the comparison with **Y-1**, amide remained as linkage group L.

Q fragment was investigated on rigid and steric factors. **I-04** exhibited significant loss of kinase inhibitory potency. This result was attributed to the effect of π - π hyperconjugation between the cyclopropyl C-C bonds and the amide C=O exerting a conformational bias based on the increased π character of cyclopropyl C-C bonds which can optimally interact with the amide C=O moiety at 0° and 180° (the Thorpe-Ingold effect).²⁸ Moreover, the 116 bond angle enforced by the cyclopropyl

ring is closer to the 120 vector inherent to the pyridine core. Expanding the cyclopropyl of **I-01** to cyclopentyl of **I-05** resulted in significant loss of kinase inhibitory potency. The cyclopentyl ring also didn't provide for the aforementioned electronic stabilization (hyperconjugation) that the cyclopropyl analogs provide. **I-01** using amide group and cyclopropyl as L and Q displayed optimal enzymatic activity.

We hypothesized that the poor antiproliferative activity of **I-01** against A375 cell lines ($IC_{50} = 18.4 \mu\text{M}$) was due to its meager solubility and cellular permeability. In order to get a better occupation of the solvent accessible region proximal to the pyrimidine ring, we introduced the solubilizing functional group R^1 . **I-06~I-22** increased in solubilities, compared to those analogs **I-01~I-05** lacking solubility enhancing functional group at R^1 (Solubility determination was presented in supporting information).²⁹ The goal to ameliate solubility was achieved with analog **I-15**, achieving solubility of 0.228 mg/mL (Table 1).

Different steric size of R^1 was explored. We envisioned introduction of hydroxyl, methoxyl or amino functional group through carbon linker into pyrimidine ring. It has been reported that the presence of these groups can properly occupy the solvent accessible region.³⁰⁻³² **I-06~I-08** weren't achieve apparent change of enzymatic activity. Secondary amine **I-09** was introduced through a two-carbon linker at the pyrimidine ring, which resulted in loss of $\text{BRaf}^{\text{V600E}}$ inhibition. Compared to **I-09**, the enzymatic activity of **I-10** was significantly increased. This result confirmed the importance of the tertiary amine for Raf kinase activity. Due to steric compatibility with $\text{BRaf}^{\text{V600E}}$, expanding the tertiary amine of **I-10** to cyclic amine of **I-11** resulted in 2-fold increase in enzymatic activity.

The effect of increasing the length of the linker carbon chain bearing the solubilizing amino functional group was explored. When the linker carbon length was increased from two carbons to three carbons (**I-07 to I-08**, **I-11 to I-12**), the enzymatic activity decreased. The linker of two carbons was better suited for hydrophilic interactions. Based on this information, cyclic tertiary amines pyrrolidine, piperidine and N-methylpiperazine were introduced to pyrimidine through two carbons chain to achieve **I-13~I-15**. Compared to **I-01**, they increased enzymatic activity. Especially,

I-15 displayed 6-fold increase of enzymatic activity compared to **I-01**, with IC_{50} value as 12.6 nM. This result showed that the steric accommodation was the core factor for R^1 to affect enzymatic activity. Bulky groups could get a better occupation of solvent accessible region proximal to the hinge moiety of pyrimidine.

I-18 was removed of lipophilic groups trifluoromethyl ($-CF_3$) to afford **I-19**. The loss of enzymatic activity indicated that R^2 substituent was necessary for enzymatic potency. As described above, R^3 toward another solvent accessible region. The modification introducing solubilizing functional groups at R^3 position afforded **I-16~I-22** to get a better occupation of solvent accessible region. Perhaps due to not occupy the solvent accessible region properly, **I-16~I-22** resulted in significantly decreased enzymatic activity. **I-18**, **I-20** and **I-22** were tolerated.

2.3.2. The Pan-Raf activity of chosen compounds

As mentioned earlier, Pan-Raf inhibitors with similar activity against all subtypes of Raf proteins might have potential to overcome the resistance caused by vemurafenib. The Raf protomer IC_{50} values of chosen compounds were comparable to vemurafenib and sorafenib, especially against BRaf^{V600E} and CRaf. Although their poency weren't comparable to LY3009120 as shown in Table 2, their potency in terms of CRaf were all superior to vemurafenib.

Table 2. The Raf protomer activity of chosen compounds

Compd	IC_{50} (nM) ^a			
	BRaf ^{V600E}	ARaf	BRaf ^{WT}	CRaf
I-01	77.2±2.4	194.6±3.8	287.2±9.1	43.4±1.1
I-10	75.3±7.3	108.2±5.5	121.4±13.3	41.7±3.7
I-13	59.6±13.1	92.4±9.7	102.3±20.3	47.2±7.6
I-14	48.8±7.9	71.4±4.7	68.1±14.0	38.8±2.5
I-15	12.6±15.8	30.1±7.0	19.7±19.4	17.5±6.8
vemurafenib	31.6±2.4	2.1±0.6	6.9±8.5	135.7±0.9
sorafenib	38.1±3.0	7.1±1.1	22.6±10.4	6.2±1.3
LY3009120	5.5±3.9	1.2±2.2	1.5±12.1	3.8±0.5

^a n=3

Kinase Activity Measurement Using KiNativ Assays of ActivX Biosciences Inc.

Whole cell KiNativ assays were developed by ActivX Biosciences Inc, using whole cell lysates of A375 cells as described (Table 3).³³ **I-15** bound ARaf, BRaf, and CRaf native proteins with IC₅₀ values of 284, 168–225, and 163 nM, respectively. Vemurafenib was able to bind to BRaf and ARaf with IC₅₀ values of 280–320 and 1130 nM, respectively; however, its binding affinity to CRaf was greater than 10,000 nM. LY3009120 bound ARaf, BRaf, and CRaf potently with IC₅₀ values of 44, 31–47, and 42 nM respectively.

Table 3. Raf KiNativ data in A375 cells

Compd	IC ₅₀ (nM)		
	ARaf	BRaf	CRaf
I-15	284	168-225	163
vemurafenib	1130	280-320	>10000
LY3009120	44	31-47	42 ^a

^a Cite the reference 15

Although the potency of **I-15** wasn't comparable to LY3009120, its potency was superior to vemurafenib.

2.4. Antiproliferative activity against different cell lines in vitro

As described above, all isoforms of Raf are important targets in developing small-molecular inhibitors for cancer therapies, especially melanoma, colon cancer and hepatoma.³⁴ A375,³⁵ and COLO-205³⁶ cell lines have extraordinary expression of BRaf^{V600E}. SK-Mel-2²³ and HepG2 cell lines have extraordinary expression of BRaf^{WT}.³⁷

Antiproliferative activities of compounds with good enzymatic activity against A375, SK-Mel-2, COLO-205 and HepG2 cell lines were evaluated. The results were summarized in Figure 6.

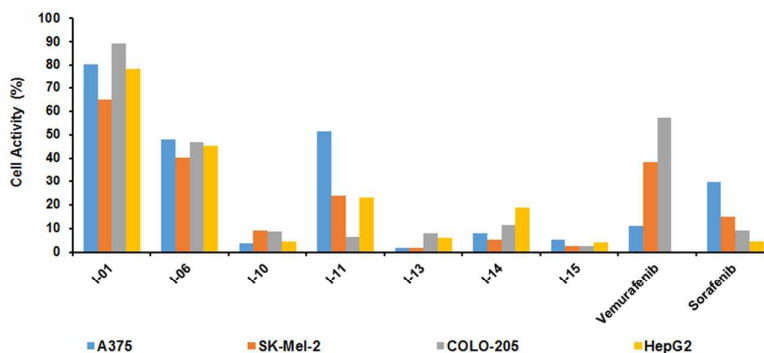


Figure 6. The cellular potency of compounds against cell lines with concentration of 10 μM

Introducing hydroxyl group through carbon linker at the pyrimidine ring to achieve **I-06** resulted in improved potency against all the cell lines compared to **I-01** (The solubility was improved from 0.016 mg/mL of **I-01** to 0.102 mg/mL of **I-06**). Then, various tertiary amines of different steric sizes were explored. Initially, **I-10** with N, N-dimethyl amino substitution displayed significantly increased cellular potency compared to **I-06**. Subsequently, **I-11** and **I-13~I-15** with cyclic tertiary amines were investigated. **I-13~I-15** were superior to **I-10**, while **I-11** wasn't comparable to **I-10**. This result displayed that the cyclic tertiary amines would be better suited to increase cellular potency. Eventually, the chosen compounds with good antiproliferative activity were tested on the cell lines to acquire the IC_{50} values. The data showed in Table 4.

Table 4. The IC_{50} values of chosen compounds against various cell lines

Compd	IC_{50} (μM) ^a			
	A375	COLO-205	SK-Mel-2	HepG2
I-10	3.26±0.41	3.36±0.62	2.31±0.10	4.52±0.13
I-13	2.37±0.17	3.95±1.48	1.92±0.56	3.67±0.94
I-14	1.78±0.38	3.62±0.66	1.54±0.72	2.13±0.70
I-15	1.07±0.10	1.92±0.34	0.58±0.04	2.46±0.11
vemurafenib	0.70±0.09	5.16±1.39	5.64±1.07	5.48±1.01
sorafenib	13.64±2.44	7.04±0.87	11.35±2.10	2.84±0.41

LY3009120	0.31±0.09	0.96±0.13	0.22±0.03	2.60±0.91
-----------	-----------	-----------	-----------	-----------

^an=5

The antiproliferative activity of **I-10** and **I-13~I-15** against A375 and HepG2 cell lines were comparable to vemurafenib and sorafenib. When tested on SK-Mel-2 and COLO-205, their potency proved to be superior to vemurafenib and sorafenib. Overall, all the compounds bearing solubilizing functional group showed improved cellular potency compared to **I-01**. Interestingly, within this series of compounds, cellular potencies followed roughly the same rank order of biochemical potencies. The improved cellular activity is probably due to enhanced solubility.

It should be noted that **I-14** and **I-15** had a similar Pan-Raf activity and various cellular potency as that of the compounds vemurafenib and sorafenib.

Although **I-15** wasn't comparable to LY3009120 against A375 cell line, its potencies against COLO-205, SK-Mel-2 and HepG2 cell lines were comparable.

2.5. Research on biological mechanisms

We tested **I-14** and **I-15** for its ability to inhibit P-ERK in cancer cells by Western blot analysis (Figure 7). **I-14** and **I-15** effectively and dose-dependently inhibits P-ERK in the A375 cell line with BRaf^{V600E} at concentration as low as 400 nM, which is as potent as vemurafenib. In the SK-Mel-2 cell line with BRaf^{WT}, **I-14** and **I-15** effectively and dose-dependently inhibits P-ERK at concentration as low as 400 nM, too. However, vemurafenib activates P-ERK with the increase of its concentration.

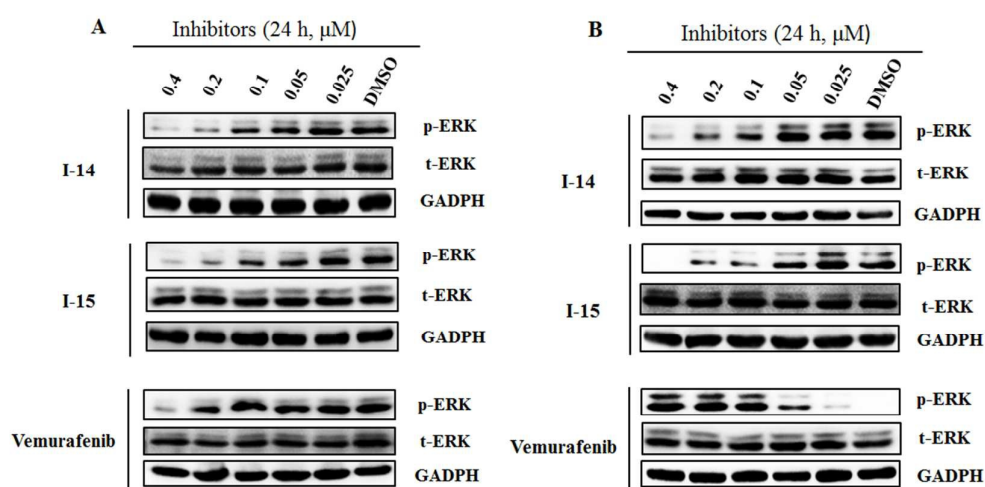


Figure 7. (A) ERK kinase inhibition in A375 (B) ERK kinase inhibition in SK-Mel-2

Our results supported that Pan-Raf inhibition might be a tractable strategy to overcome the intrinsic or acquired resistance of melanoma cancer caused by vemurafenib.

2.6. Research on pharmacokinetics behavior

The favorable in vitro profiles prompted us to evaluate **I-15** in vivo, compared to **Y-1**. The pharmacokinetic (PK) parameters of **Y-1** and **I-15** were assessed in male SD rat following intravenous (IV) and oral (PO) administrations as described in Table 5 and Table 6.

I-15 possesses favorable pharmacokinetic profiles with high oral exposures ($AUC_{0-\infty}$) of over 868.0 $\mu\text{g/L}\cdot\text{h}$ at a 10 mg/kg oral dose and acceptable half-life ($T_{1/2} = 5.9$ h). After IV administration **I-15** at a dose of 2.5 mg/kg, maximum concentration (C_{max}) reached 127.5 $\mu\text{g/L}$, and area under the curve ($AUC_{0-\infty}$) was 695.7 $\mu\text{g/L}\cdot\text{h}$. After oral administration at 10 mg/kg, C_{max} reached 68.5 $\mu\text{g/L}$ at 6.0 h post dosing. These results demonstrate good pharmacokinetic properties of **I-15** in rat with high oral bioavailability $F = 33.4\%$ and a sustained plasma concentration exceeding in vitro EC_{50} during at least 11.8 h after oral dosing. **I-15** also exhibited low clearance (CL) and high volume of distribution (V_{ss}).

Table 5. Pharmacokinetic profile of **Y-1** in rat

PK parameters (n=3)	IV (2.5 mg/Kg)	SD	PO (10 mg/Kg)	SD
$AUC_{(0-t)}$ (ug.h/L)	378.4	58.3	509.1	87.3
$AUC_{(0-\infty)}$ (ug.h/L)	405.8	90.1	590.6	75.6
$t_{1/2}$ (h)	8.3	2.1	7.3	1.7
T_{max} (h)	0.083	0.1	4.0	1.9
CL (L/h/Kg)	6.2	1.2	N/A	1.8
V (L/Kg)	73.4	7.6	N/A	32.5
C_{max} (ug/L)	225.0	28.8	68.9	23.4
F			33.6	6.0

Table 6. Pharmacokinetic profile of **I-15** in rat

PK parameters (n=3)	IV (2.5 mg/Kg)	SD	PO (10 mg/Kg)	SD
$AUC_{(0-t)}$ (ug.h/L)	600.4	37.4	801.2	45.2
$AUC_{(0-\infty)}$ (ug.h/L)	695.7	57.1	868.0	38.7

$t_{1/2}$ (h)	7.3	1.5	5.9	0.9
T_{max} (h)	0.083	0	6.0	0.9
CL (L/h/Kg)	3.6	1.1	N/A	2.9
V (L/Kg)	37.7	8.2	N/A	25.5
C_{max} (ug/L)	127.5	16.8	68.5	6.2
F (%)			33.4	5.2

N/A ^a: not applicable

The Plasma Concentration-time curve of **Y-1** and **I-15** was shown in Figure 8, the experimental process was presented in Experimental section (see Supporting Information).

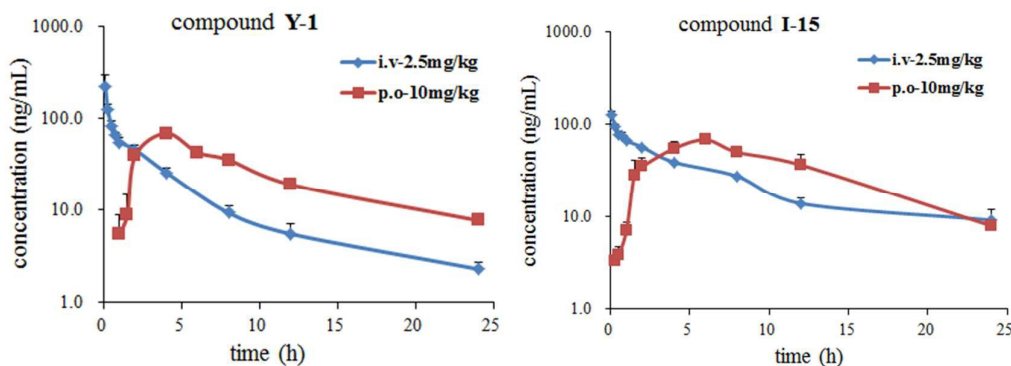


Figure 8. The Plasma Concentration-time curve of **Y-1** and **I-15**

From the Plasma Concentration-time curve, we know the $AUC_{0-\infty}$ value of **Y-1** was lower than **I-15**. The SD value of **Y-1** was higher than **I-15**, too. These data indicate a favorable pharmacokinetic profile of **I-15** in preparation for efficacy studies in rat.

3. Conclusion

Our previous studies toward targeted anticancer agents have included the discovery of **Y-1**. Replacing the purine group in hinge moiety of **Y-1** by pyrimidine group results in **I-01** as a novel Pan-Raf inhibitory template, which inhibits all subtypes of Raf protomer proteins with IC_{50} values as 77.2 nM (BRaf^{V600E}), 194 nM (ARaf), 287 nM (BRaf^{WT}) and 43.4 nM (CRaf), respectively. On the basis of information obtained from the binding mode of **I-01**, various solubilizing functional groups as R¹ and R³ group were introduced to 4-position pyrimidine ring in hinge moiety or terminal phenyl to achieve a better occupation of solvent accessible region, and this optimization campaign lead to the identification of **I-15** as a Pan-Raf inhibitor with

improved solubility. As the representative compound, **I-15** inhibited all subtypes of Raf protomer with IC₅₀ values of 12.6 nM (BRaf^{V600E}), 30.1 nM (ARaf), 19.7 nM (BRaf^{WT}) and 17.5 nM (CRaf), respectively. Although **I-15** wasn't comparable with LY3009120 in terms of cellular potency, its potency was superior to or comparable with vemurafenib and sorafenib (The selected cell lines were extraordinarily expressed BRAF^{V600E} or BRaf^{WT}). The western blot results for the P-ERK inhibition in human melanoma A375 and SK-Mel-2 cell lines displayed our compounds inhibited the proliferation of A375 cell lines through ERK pathway, without paradoxical activation of ERK in SK-Mel-2 cell lines. Our results supported the hypothesis that the Pan-Raf inhibition might be a tractable strategy to overcome the acquired resistance caused by vemurafenib. The better pharmacokinetics profile in rat proved **I-15** was suitable in preparation for efficacy studies in rat. Thus **I-15** was a promising lead compound to be developed as a potent Pan-Raf inhibitor.³⁸⁻⁴²

4. Experimental section

4.1. Molecular docking and fragment-based strategy

Crystal structures of BRaf^{V600E} (PDB 3IDP) were downloaded from Protein Data Bank (PDB) and prepared by the Protein Preparation Wizard in the Schrödinger suite.⁴³ All compounds were initially minimized by the LigPrep module. Due to its excellent performance through a self-docking analysis,⁴⁴ the Glide module (extra precision [XP] mode) was selected for molecular docking and the top 10 poses of each ligand were minimized by a post docking program with the best pose saved for further analysis. In the fragment-based strategy, detailed decomposition of the compound databases was found in a method proposed before²⁵ and the RECAP algorithm were implemented in Pipeline Pilot 7.5 with the Generate Recap Fragments protocol.²⁶ Duplications were removed no matter for decomposing or resynthesing compounds.

Acknowledgments

This work was financially supported by National Natural Science Foundation of China (No. 21572273/ B020601), A Project Funded by the Priority Academic Program Development of Jiangsu Higher Education Institutions and College Student

Innovation Project for the R&D of Novel Drugs (No. J1030830). We also express our gratitude to Dr. Xiazhong Ren, Dr. Huajun Yang, Dr. Chunlan Dong (Crown Bioscience Corporation) and Dr. Jamie Planck (RBC, Pennsylvania, USA) for their helpful support in biological evaluation.

Notes and References

1. G. Maik-Rachline and R. Seger, *Drug Resist. Updat.*, 2016, 25, 1-12.
2. H. Lavoie and M. Therrien, *Nature reviews. J. Mol. Cell Biol.*, 2015, 16, 281-298.
3. A. P. Rebocho and R. Marais, *Oncogene*, 2013, 32, 3207-3212.
4. J. Mooz, T. K. Oberoi-Khanuja, G. S. Harms, W. Wang, B. S. Jaiswal, S. Seshagiri, R. Tikkanen and K. Rajalingam, *Sci. Signal.*, 2014, 7, ra73.
5. A. P. Rebocho and R. Marais, *Cancer Discov.*, 2011, 1, 98-99.
6. P. T. C. Wan, M. J. Garnett, S. M. Roe, S. Lee, D. Niculescu-Duvaz, V. M. Good, C. G. Project, C. M. Jones, C. J. Marshall, C. J. Springer, D. Barford and R. Marais, *Cell*, 2004, 116, 855-867.
7. X. Wang and J. Kim, *J. Med. Chem.*, 2012, 55, 7332-7341.
8. A. Backes, B. Zech, B. Felber, B. Klebl and G. Muller, *Expert Opin. Drug Discov.*, 2008, 3, 1427-1449.
9. J. R. Henry, M. D. Kaufman, S. B. Peng, Y. M. Ahn, T. M. Caldwell, L. Vogeti, H. Telikepalli, W. P. Lu, M. M. Hood, T. J. Rutkoski, B. D. Smith, S. Vogeti, D. Miller, S. C. Wise, L. Chun, X. Zhang, Y. Zhang, L. Kays, P. A. Hipskind, A. D. Wroblewski, K. L. Lobb, J. M. Clay, J. D. Cohen, J. L. Walgren, D. McCann, P. Patel, D. K. Clawson, S. Guo, D. Manglicmot, C. Groshong, C. Logan, J. J. Starling and D. L. Flynn, *J. Med. Chem.*, 2015, 58, 4165-4179.
10. G. A. McArthur, P. B. Chapman, C. Robert, J. Larkin, J. B. Haanen, R. Dummer, A. Ribas, D. Hogg, O. Hamid, P. A. Ascierto, C. Garbe, A. Testori, M. Maio, P. Lorigan, C. Lebbé, T. Jouary, D. Schadendorf, S. J. O'Day, J. M. Kirkwood, A. M. Eggermont, B. Dréno, J. A. Sosman, K. T. Flaherty, M. Yin, I. Caro, S. Cheng, K. Trunzer and A. Hauschild, *Lancet Oncol.*, 2014, 15, 323-332.
11. K. T. Flaherty, I. Puzanov, K. B. Kim, A. Ribas, G. A. McArthur, J. A. Sosman, P. J. O'Dwyer, R. J. Lee, J. F. Grippo, K. Nolop and P. B. Chapman, *N. Engl. J. Med.*, 2010, 363, 809-819.
12. P. B. Chapman, A. Hauschild, C. Robert, J. B. Haanen, P. Ascierto, J. Larkin, R. Dummer, C. Garbe, A. Testori and M. Maio, *N. Engl. J. Med.*, 2011, 364, 2507-2516.
13. A. Hauschild, J.-J. Grob, L. V. Demidov, T. Jouary, R. Gutzmer, M. Millward, P. Rutkowski, C. U. Blank, W. H. Miller, E. Kaempgen, S. Martín-Algarra, B. Karaszewska, C. Mauch, V. Chiarion-Sileni, A.-M. Martin, S. Swann, P. Haney, B. Mirakhur, M. E. Guckert, V. Goodman and P. B. Chapman, *Lancet*, 2012, 380, 358-365.
14. S.-B. Peng, James R. Henry, Michael D. Kaufman, W.-P. Lu, Bryan D. Smith, S. Vogeti, Thomas J. Rutkoski, S. Wise, L. Chun, Y. Zhang, Robert D. Van Horn, T. Yin, X. Zhang, V. Yadav, S.-H. Chen, X. Gong, X. Ma, Y. Webster, S. Buchanan, I.

- Mochalkin, L. Huber, L. Kays, G. P. Donoho, J. Walgren, D. McCann, P. Patel, I. Conti, Gregory D. Plowman, James J. Starling and Daniel L. Flynn, *Cancer Cell*, 2015, 28, 384-398.
15. J. R. Henry, M. D. Kaufman, S.-B. Peng, Y. M. Ahn, T. M. Caldwell, L. Vogeti, H. Telikepalli, W.-P. Lu, M. M. Hood, T. J. Rutkoski, B. D. Smith, S. Vogeti, D. Miller, S. C. Wise, L. Chun, X. Zhang, Y. Zhang, L. Kays, P. A. Hipskind, A. D. Wroblewski, K. L. Lobb, J. M. Clay, J. D. Cohen, J. L. Walgren, D. McCann, P. Patel, D. K. Clawson, S. Guo, D. Manglicmot, C. Groshong, C. Logan, J. J. Starling and D. L. Flynn, *J. Med. Chem.*, 2015, 58, 4165-4179.
16. S.-H. Chen, Y. Zhang, R. D. Van Horn, T. Yin, S. Buchanan, V. Yadav, I. Mochalkin, S. S. Wong, Y. G. Yue, L. Huber, I. Conti, J. R. Henry, J. J. Starling, G. D. Plowman and S.-B. Peng, *Cancer Discov.*, 2016, 6, 300.
17. B. Sanchez-Laorden, A. Viros, M. R. Girotti, M. Pedersen, G. Saturno, A. Zambon, D. Niculescu-Duvaz, S. Turajlic, A. Hayes, M. Gore, J. Larkin, P. Lorigan, M. Cook, C. Springer and R. Marais, *Sci. Signal.*, 2014, 7, ra30.
18. S. J. Heidorn, C. Milagre, S. Whittaker, A. Nourry, I. Niculescu-Duvas, N. Dhomen, J. Hussain, J. S. Reis-Filho, C. J. Springer, C. Pritchard and R. Marais, *Cell*, 2010, 140, 209-221.
19. P. I. Poulikakos, C. Zhang, G. Bollag, K. M. Shokat and N. Rosen, *Nature*, 2010, 464, 427-430.
20. G. Hatzivassiliou, K. Song, I. Yen, B. J. Brandhuber, D. J. Anderson, R. Alvarado, M. J. Ludlam, D. Stokoe, S. L. Gloor, G. Vigers, T. Morales, I. Aliagas, B. Liu, S. Sideris, K. P. Hoeflich, B. S. Jaiswal, S. Seshagiri, H. Koeppen, M. Belvin, L. S. Friedman and S. Malek, *Nature*, 2010, 464, 431-435.
21. R. Arora, M. Di Michele, E. Stes, E. Vandermarliere, L. Martens, K. Gevaert, E. Van Heerde, J. T. Linders, D. Brehmer, E. Jacoby and P. Bonnet, *J. Med. Chem.*, 2015, 58, 1818-1831.
22. M. Okaniwa, M. Hirose, T. Arita, M. Yabuki, A. Nakamura, T. Takagi, T. Kawamoto, N. Uchiyama, A. Sumita, S. Tsutsumi, T. Tottori, Y. Inui, B. C. Sang, J. Yano, K. Aertgeerts, S. Yoshida and T. Ishikawa, *J. Med. Chem.*, 2013, 56, 6478-6494.
23. A. Nakamura, T. Arita, S. Tsuchiya, J. Donelan, J. Chouitar, E. Carideo, K. Galvin, M. Okaniwa, T. Ishikawa and S. Yoshida, *Cancer Res.*, 2013, 73, 7043-7055.
24. W. Yang, Y. Chen, X. Zhou, Y. Gu, W. Qian, F. Zhang, W. Han, T. Lu and W. Tang, *Eur. J. Med. Chem.*, 2015, 89, 581-596.
25. Y. Zhang, Y. Jiao, X. Xiong, H. Liu, T. Ran, J. Xu, S. Lu, A. Xu, J. Pan, X. Qiao, Z. Shi, T. Lu and Y. Chen, *Mol. Divers.*, 2015, 19, 895-913.
26. Y. Yaxia, P. Jianfeng and L. Luhua, *Curr. Pharm. Des.*, 2013, 19, 2326-2333.
27. R. M. Anforth, T. C. Blumetti, R. F. Kefford, R. Sharma, R. A. Scolyer, S. Kossard, G. V. Long and P. Fernandez-Penas, *Br. J. Dermatol.*, 2012, 167, 1153-1160.
28. N. A. Meanwell, *J. Med. Chem.*, 2011, 54, 2529-2591.
29. A. Mallinger, K. Schiemann, C. Rink, F. Stieber, M. Calderini, S. Crumpler, M. Stubbs, O. Adeniji-Popoola, O. Poeschke, M. Busch, P. Czodrowski, D. Musil, D. Schwarz, M.-J. Ortiz-Ruiz, R. Schneider, C. Thai, M. Valenti, A. de Haven Brandon,

- R. Burke, P. Workman, T. Dale, D. Wienke, P. A. Clarke, C. Esdar, F. I. Raynaud, S. A. Eccles, F. Rohdich and J. Blagg, *J. Med. Chem.*, 2016, 59, 1078-1101.
30. A. Poulsen, S. Blanchard, C. K. Soh, C. Lee, M. Williams, H. Wang and B. Dymock, *Bioorg. Med. Chem. Lett.*, 2012, 22, 305-307.
31. A. A. Mortlock, K. M. Foote, N. M. Heron, F. H. Jung, G. Pasquet, J.-J. M. Lohmann, N. Warin, F. Renaud, C. De Savi, N. J. Roberts, T. Johnson, C. B. Dousson, G. B. Hill, D. Perkins, G. Hatter, R. W. Wilkinson, S. R. Wedge, S. P. Heaton, R. Odedra, N. J. Keen, C. Crafter, E. Brown, K. Thompson, S. Brightwell, L. Khatri, M. C. Brady, S. Kearney, D. McKillop, S. Rhead, T. Parry and S. Green, *J. Med. Chem.*, 2007, 50, 2213-2224.
32. J. J. Cui, M. Tran-Dubé, H. Shen, M. Nambu, P.-P. Kung, M. Pairish, L. Jia, J. Meng, L. Funk, I. Botrous, M. McTigue, N. Grodsky, K. Ryan, E. Padrique, G. Alton, S. Timofeevski, S. Yamazaki, Q. Li, H. Zou, J. Christensen, B. Mroczkowski, S. Bender, R. S. Kania and M. P. Edwards, *J. Med. Chem.*, 2011, 54, 6342-6363.
33. Matthew P. Patricelli, Tyzoon K. Nomanbhoy, J. Wu, H. Brown, D. Zhou, J. Zhang, S. Jagannathan, A. Aban, E. Okerberg, C. Herring, B. Nordin, H. Weissig, Q. Yang, J.-D. Lee, Nathanael S. Gray and John W. Kozarich, *Chem. Biol.*, 2011, 18, 699-710.
34. G. Maurer, B. Tarkowski and M. Baccarini, *Oncogene*, 2011, 30, 3477-3488.
35. A. E. Gould, R. Adams, S. Adhikari, K. Aertgeerts, R. Afroze, C. Blackburn, E. F. Calderwood, R. Chau, J. Chouitar, M. O. Duffey, D. B. England, C. Farrer, N. Forsyth, K. Garcia, J. Gaulin, P. D. Greenspan, R. Guo, S. J. Harrison, S. C. Huang, N. Iartchouk, D. Janowick, M. S. Kim, B. Kulkarni, S. P. Langston, J. X. Liu, L. T. Ma, S. Menon, H. Mizutani, E. Paske, C. C. Renou, M. Rezaei, R. S. Rowland, M. D. Sintchak, M. D. Smith, S. G. Stroud, M. Tregay, Y. Tian, O. P. Veiby, T. J. Vos, S. Vyskocil, J. Williams, T. Xu, J. J. Yang, J. Yano, H. Zeng, D. M. Zhang, Q. Zhang and K. M. Galvin, *J. Med. Chem.*, 2011, 54, 1836-1846.
36. S. Mathieu, S. N. Gradl, L. Ren, Z. Wen, I. Aliagas, J. Gunzner-Toste, W. Lee, R. Pulk, G. Zhao, B. Aliche, J. W. Boggs, A. J. Buckmelter, E. F. Choo, V. Dinkel, S. L. Gloor, S. E. Gould, J. D. Hansen, G. Hastings, G. Hatzivassiliou, E. R. Laird, D. Moreno, Y. Ran, W. C. Voegtli, S. Wenglowsky, J. Grina and J. Rudolph, *J. Med. Chem.*, 2012, 55, 2869-2881.
37. M. Xing, W. H. Westra, R. P. Tufano, Y. Cohen, E. Rosenbaum, K. J. Rhoden, K. A. Carson, V. Vasko, A. Larin, G. Tallini, S. Tolaney, E. H. Holt, P. Hui, C. B. Umbricht, S. Basaria, M. Ewertz, A. P. Tufaro, J. A. Califano, M. D. Ringel, M. A. Zeiger, D. Sidransky and P. W. Ladenson, *J. Clin. Endocrinol. Metab.*, 2005, 90, 6373-6379.
38. A. T. Mavrova, S. Dimov, D. Yancheva, M. Rangelov, D. Wesselinova and J. A. Tsenov, *Eur. J. Med. Chem.*, 2016, 123, 69-79.
39. A. K. El-Damasy, J.-H. Lee, S. H. Seo, N.-C. Cho, A. N. Pae and G. Keum, *Eur. J. Med. Chem.*, 2016, 115, 201-216.
40. V. Asati, D. K. Mahapatra and S. K. Bharti, *Eur. J. Med. Chem.*, 2016, 109, 314-341.
41. Y. Chen, Y. Zheng, Q. Jiang, F. Qin, Y. Zhang, L. Fu and G. He, *Eur. J. Med.*

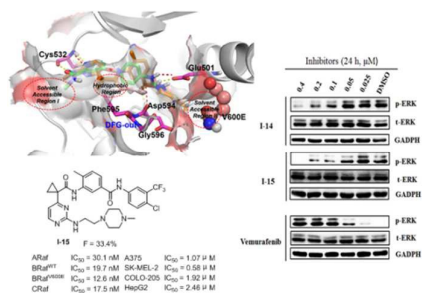
Chem., 2017, 127, 997-1011.

42. M. M. Mohyeldin, B. A. Busnena, M. R. Akl, A. M. Dragoi, J. A. Cardelli and K. A. El Sayed, *Eur. J. Med. Chem.*, 2016, 118, 299-315.

43. L. Schrodinger, New York: Schrödinger, LLC, 2011.

44. Y. Zhang, S. Yang, Y. Jiao, H. Liu, H. Yuan, S. Lu, T. Ran, S. Yao, Z. Ke, J. Xu, X. Xiong, Y. Chen and T. Lu, *J. Chem. Inf. Model.*, 2013, 53, 3163-3177.

For Table of Contents Use Only



Highlight

Describe the design and characterization of a series of pyrimidine scaffold as Pan-Raf inhibitors, which may overcome the resistance associated with current BRaf^{V600E} inhibitors.